Optics & Laser Technology 42 (2010) 301–307

Contents lists available at ScienceDirect

Optics & Laser Technology

journal homepage: www.elsevier.com/locate/optlastec

Diode laser spectrally fixed at an atomic absorption line

Margarita Deneva [a,*], Elena Stoykova [a,b], Marin Nenchev [a,1], Rene Barbe [a], Jean-Claude Keller [a]

[a] Laboratoire de Physique des Lasers, Institut Galilee, Universite Paris-Nord, 93430 Villetaneuse, France
[b] Central laboratory of Optical Storage and Processing of Information, Bulgarian Academy of Sciences, Acad. Georgi Bonchev Str. Bl.101, 1113 Sofia, Bulgaria

ARTICLE INFO

Article history:
Received 15 December 2008
Received in revised form
12 July 2009
Accepted 15 July 2009
Available online 20 August 2009

Keywords:
Diode laser
Reference atomic line
Spectrum fixation

ABSTRACT

A simple all-optical technique for fixing the spectrum of the output from semiconductor laser at a chosen absorption atomic line is realized and studied. The technique, which is not of a laser locking type, uses a conventional diode laser without any influence on its operation. For implementation of the technique, the diode laser output is fed to a modified Michelson interferometer, and controllable disturbing of phase and amplitude correlation between the interfering beams in the two arms of the interferometer is achieved by frequency scanning through a contour of a reference absorption line of a substance introduced in one of the arms of the interferometer. It is shown both by experiment and theory that, under properly chosen conditions, the spectrum of the obtained light is fixed at the atomic line and has a linewidth comparable to the linewidth of the used absorption line.

1. Introduction

High efficiency, good power stability, wide wavelength coverage and tunability, high reliability and low-cost are the features which have established the modern semiconductor diode laser as a versatile tool for a variety of applications. Laser spectroscopy, optical frequency synthesis, atomic physics and metrology are the areas of their frequent utilization [1–4]. Diode lasers serve as highly reliable frequency standards for wavelength division multiplexed systems in optical communications [5]. The potential of diode lasers is still to be exploited in laser isotope separation systems [6] and differential absorption lidar [7,8].

Spectral control in diode lasers by locking to a reference atomic or molecular absorption line has attracted a lot of research effort over the last two decades [e.g. 9–34]. The techniques under most active development in this field are of the so called "mode locking" type [9–34]. Actually, the term unites two large groups of approaches. The first group implements the mode locking by using a tunable spectrally selective laser and an external opto-electronic sub-system to compare the laser spectrum with a reference absorption line as well as a servo-system to provide a feedback control of the laser emission [10–27]. The essential drawback of these systems is their technical complexity and hence, expensive realization due to incorporation of additional subsystems and elements for spectral control. The second group of approaches relies on different physical phenomena to influence the laser operation to achieve the locking [9,23]. The systems which are built following these two approaches, and especially the first as traditionally employed, can produce very narrow linewidths with a high factor of frequency stabilization. Typical for operation of these laser systems, and being a general problem for all resonator intervention (extra-, or intraresonator) locking techniques, is the strong dependence of the laser output on small and, respectively, difficult to control variations in the gain, losses, temperature, or on inevitable resonator misalignment caused by mechanical vibrations, electric and magnetic fields. Both technical complexity and stability constraints make the mode-locked laser systems rather cumbersome and sophisticated equipment to be utilized for routine spectroscopic and metrological measurements. There are many tasks with less stringent requirements on the emission linewidth that do not need such high-precision systems. For example, a frequently encountered task in spectroscopy or isotope separating experiments is an excitation of transition which belongs to a particular substance in a mixture of different substances, e.g. Cs, Rb or some other substance in a gas mixture. The only requirement of the diode laser system which should solve this task would be to ensure a narrow enough output to act only on the desired transition.

In the present paper, we propose and check, both by theory and experiment implementation, a simple non-locking type technique for production of a pulsed diode laser emission, which is spectrally fixed at the wavelength of a desired atomic absorption transition. The emitted laser light at the output of the proposed system is fixed at the reference line in a purely optical way without any influence on the diode laser operation. A standard

* Correspondence to: Deneva M., Technical University-Sofia, Branch Plovdiv, 25 Tsanko Dustabanov Str., 4000 Plovdiv, Bulgaria.
E-mail addresses: mdeneva@yahoo.com, deneva@tu-plovdiv.bg (M. Deneva), elena@optics.bas.bg (E. Stoykova).
[1] Permanent address: Institute of Electronics, Bulgarian Academy of Sciences, 72 Tsarigradsko Shosse Blvd., 1784 Sofia, Bulgaria.

0030-3992/$ - see front matter © 2009 Elsevier Ltd. All rights reserved.
doi:10.1016/j.optlastec.2009.07.008

single-mode diode laser tuned by variation of the exciting current can be used, and no spectrally selective elements or comparative electronics are required. This essentially simplifies laser control and decreases the influence of external electric, magnetic and radiation fields. The system permits a distant control (up to ten meters from the diode source).

The developed technique relies on feeding the diode laser output into a modified Michelson interferometer and the controllable disturbance of the phase and amplitude correlation between the two interfering beams under frequency scanning through a reference absorption line which belongs to a substance introduced in one of the arms of the interferometer. The unbalance is produced by the absorption and the refractive index change throughout the contour of the absorption line. The control of the unbalance is realized by variation of the optical path length in the other arm of the interferometer through an appropriate tilting of a glass plate introduced in this arm. This type of approach, but without control, has been previously used in spectroscopy for measurement of the variation of gas refractive indices [33,34] with a dye laser [33] and a gas-discharge lamp [34].

2. Experimental arrangement

Our experimental set-up is shown in Fig. 1. A commercial single longitudinal mode diode laser (DBR type, mark SDL-5702-H1) with an emission linewidth of about 100 MHz was used as a light source. The wavelength of the selected mode of the diode laser was repetitively scanned (forward–backward) within ± 10 GHz ($\sim$0.0210 nm) around the 852.1 nm Cs absorption line ($6S_{1/2}$–$6P_{3/2}$ transition). In our experiments, the scanning was performed with 100 Hz repetition rate using a laser diode driver EU-42 of Roithner Lasertechnik. The scanning repetition rate was optional and could be increased. The chosen line was a single absorption line within the scanned frequency region. The scanning was accomplished by current modulation within ± 5 around 44.3 mA. The diode temperature was kept at 17.9 °C with accuracy of ± 0.1 °C. The diode laser beam, after passing through an optical isolation system, impinged the entrance beam-splitter of a modified Michelson interferometer composed from the beam-splitter and wedged full reflecting dielectric mirrors M_1 and M_2. The isolation system can be arranged as a Faraday isolator or a combination of a polarizer and a quarter-wave plate; the latter solution was used, as is shown in Fig. 1. Both mirrors were placed at equal distances of 50 mm from the beam-splitter. The beams reflected from M_1 and M_2 interfered at the beam-splitter and formed the useful interferometer output (Output 1 in Fig. 1).

A cell with Cs atoms vapor at room temperature (22 °C) was introduced in the interferometer's first arm between the beam-splitter and mirror M_1. The length of the cell was 5 cm. The cell absorption reached about 75% for a single pass when the laser wavelength matched the maximum of 852.1 nm Cs line. An optical quality plane-parallel glass plate with thickness of $\sim$1 mm was positioned in the interferometer's second arm, i.e. between the beam-splitter and mirror M_2. The normal to the glass plate subtended a small angle θ (about one angular degree) with the impinging beam. The plate was mounted on a controllable high-precision rotary stage. The beams reflected from mirrors M_1 and M_2 subtended an angle of 7° with the corresponding incident beams. The diode laser and the interferometer were mounted on a commercial optical bench. The part of the light beam from the useful interferometer output (Output 1 in Fig. 1) was redirected to illuminate the first diode-receiver PhD_1. A wedged glass plate (the splitter SP in Fig. 1) was placed in front of the Michelson interferometer. The reflected 4% of the diode laser beam, after passing a second reference Cs cell (5 cm length, room temperature of 22 °C), illuminated the second receiver PhD_2. The measured linewidth in the reference Cs cell was $\approx$0.92 GHz (0.0019 nm, FWHM). The signals from the diode receivers were monitored using a two-channel beam oscilloscope. The oscilloscope triggering was synchronized with the scanning of the diode laser driving current.

3. Simulation of system performance

Operation of the proposed system can be briefly described as follows: as a first step, the wavelength of the diode laser is chosen by setting an appropriate value of the diode driving current close to the Cs line, but outside the region of noticeable absorption. Then, by carefully tilting of the glass plate, a completely destructive interference of the light beams from both arms of the interferometer is obtained. The de-phasing of the interfering beams at a given wavelength depends essentially on the value of the refractive indices in both arms of the interferometer and, respectively, on the variation of the optical path length introduced by the glass plate. As a result, Output 1 practically vanishes. If the wavelength of the selected mode remained outside the absorption line during the scanning of the diode driving current, the interference conditions remain the same, and the Output 1 is negligibly small. When the diode laser wavelength falls into the contour of the chosen absorption line, variation of the refractive index and the absorption change the interference conditions.

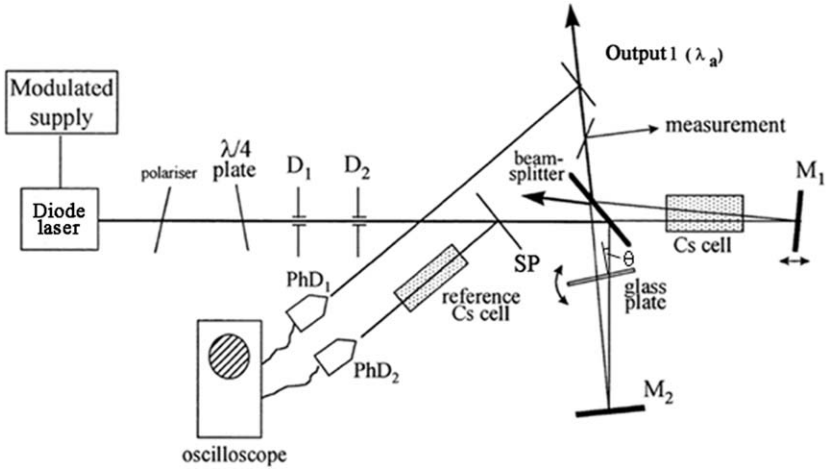

Fig. 1. Experimental set-up for spectral fixation of a diode laser light at the Cs absorption line.

Thus, the destructive interference is terminated and the interferometer Output 1 appears. Therefore, due to the scanning of the laser frequency in the frequency interval which exceeds the width of the absorption spectrum, the system operates in a "pulsed" regime.

We simulated the system operation using the theory of the Michelson interferometer [35,36]. The intensity of the beam, emitted from the interferometer Output 1, in the absence of the cell with Cs atoms and the glass plate is given by

$$I = \frac{I_0}{4}|e^{ikL_1} + e^{ikL_2}|^2 = \frac{I_0}{2}[1 + \cos(k\Delta L)] \quad (1)$$

where I_0 is the intensity which is fed to the interferometer entrance, L_1 and L_2 the geometrical path lengths of the light in the first and the second arm of the interferometer, respectively, and $k = 2\pi/\lambda$ gives the dependence on the wavelength. In the first arm of the interferometer the laser light passes twice the cell with Cs atoms, and the total phase shift and absorption upon passing through the cell can be derived from

$$\begin{aligned} E_c &= \frac{E_0}{2}\exp\{-kn_0\kappa(\Delta z + \Delta z')\}\exp\{ikn_0(\Delta z + \Delta z')\} \\ &= \frac{E_0}{2}\exp\{-kn_0\kappa(\Delta z + \Delta z')\}\exp\{ik(\Delta z + \Delta z')\} \\ &\quad \times\exp\{ik(n_0 - 1)(\Delta z + \Delta z')\} \end{aligned} \quad (2)$$

where E_0 is the amplitude of the light fed to the interferometer entrance, $n(\nu) = n_0(1+i\kappa)$ is the complex index of refraction of the cell with Cs atoms, where n_0 and κ are frequency dependent real quantities, $\nu = c/\lambda$ the linear frequency and c the velocity of light, Δz and $\Delta z'$ give the lengths of the geometrical paths of the laser light within the cell on the way to and back from the mirror M_1. If we neglect the change of the optical path introduced by refraction at the cell surfaces, we have $\Delta z' = \Delta z/\cos\varphi$, where φ is the angle between the incident and reflected beams for the mirror M_1. The expression (2) can be rewritten as

$$E_c = \frac{E_0}{2}\tau(\nu)\exp\{ik(\Delta z + \Delta z')\}\exp\{i\delta(\nu)\} \quad (3)$$

where the factor $\tau(\nu)$ describes the amplitude transmission of the cell, $\delta(\nu)$ is the phase shift introduced by the cell with Cs atoms, and the term $\exp\{ik(\Delta z+\Delta z')\}$ corresponds to free space propagation.

In the second arm of the interferometer, the laser light crosses the tilted glass plate twice. The total phase shift introduced by the plate is given by $\exp(i\phi)$ with

$$\phi = \frac{2\pi}{\lambda}h\left[n_{gl}\left(\frac{1}{\cos\theta'} + \frac{1}{\cos\theta''}\right) - \left(\frac{1}{\cos\theta} + \frac{1}{\cos(\varphi - \theta)}\right)\right], \quad (4)$$

where h is the glass plate thickness, n_{gl} its refractive index (we assume that the refractive index of the air, n_a, is equal to 1), θ is the angle between the incident laser beam and the normal to the plate surface, φ is the angle between the incident and reflected beams for the mirror M_2, its value being the same as for the mirror M_1, $\sin\theta' = {n_{gl}}^{-1}\sin\theta$ and $\sin\theta'' = {n_{gl}}^{-1}\sin(\varphi-\theta)$.

The complex amplitude of the beam, emitted from the interferometer Output 1, in the presence of the cell with Cs atoms and the glass plate is given by the expression

$$E_v = \frac{E_0}{2}[e^{ikL_1}e^{i\delta}\tau(\nu) + e^{ikL_2}e^{i\phi}] \quad (5)$$

Finally, for the intensity at Output1, we obtain

$$I(\nu) = \frac{I_0}{4}[1 + \tau^2(\nu) + 2\tau(\nu)\cos(\delta - \phi)] \quad (6)$$

where we assume that by a proper adjustment the contribution of $n_a(L_2-L_1)$ is made equal to zero.

The modeling of the system performance had two goals: the first was to check the proposed idea, and the second was to find the optimal absorption in the cesium vapor cell for achieving maximal signal output. The calculation was performed using a simplified classical atomic model [37] which is appropriate for an atomic vapor, taking into account the Doppler line broadening. The natural width of the Cs D_2 resonance line is 5 MHz [38]. Fig. 2 depicts the plots of the output intensity $I(\nu)/I_0$ within an interval of 4 GHz centered at $\nu_0 = 3.5183\times10^{14}$ Hz for the case when the phase shift introduced by the glass plate alone yields $\cos(-\phi)\cong-1$. For the purpose, we chose $h = 0.9995$ mm and $\theta = 0.0245$ rad. The obtained curves correspond to increasing density of atoms, and, hence, to increasing absorption which in figure is characterized by the value of the amplitude transmission $\tau(\lambda)$ at the center of the line ν_0. The calculated variation of the refractive index, $n_0(\nu)-1$, and the absorption, $n_0(\nu)\kappa(\nu)$, around the $6S_{1/2}-6P_{3/2}$ Cs transition at $\tau(\nu_0) = 0.05$ is presented in Fig. 3. As it can be seen from Fig. 2, the introduced phase shift ϕ leads to negligible output signal outside the contour of the absorption Cs line. In the contour of the line, the output signal has a more or less symmetrical and smooth profile at low absorption within the cell, whereas at high absorption the curves become asymmetrical and may have two peaks. However, at low absorption, the output power is halved. In general, the spectral profile of the output signal strongly depends on the angle θ. Fig. 4 gives the change in the spectral dependence of the output intensity $I(\nu)/I_0$ with $\theta = \theta_0+\Delta\theta$ for $\tau(\nu_0) = 0.11$. The calculation starts from $\theta_0 = 0.0205$, and for better comprehension the angular increment $\Delta\theta$ is given in angular minutes. We see that the desired profile of $I(\nu)/I_0$ (high intensity values close to the center of absorption line and vanishing wings outside it) is observed within a few angular minutes. This result is confirmed by Fig. 5 which shows the total power $P(\theta) = \int_{\nu_1}^{\nu_2} I(\nu)/I_0 d\nu$ at the interferometer output within the spectral interval of $\nu_2-\nu_1 = 4$ GHz as a function of θ at increasing absorption within the cell with Cs atoms. The integral is evaluated by numerical integration. The appropriate values of θ are the values close to the angle corresponding to the minimum in Fig. 5. We see that $P(\theta)$

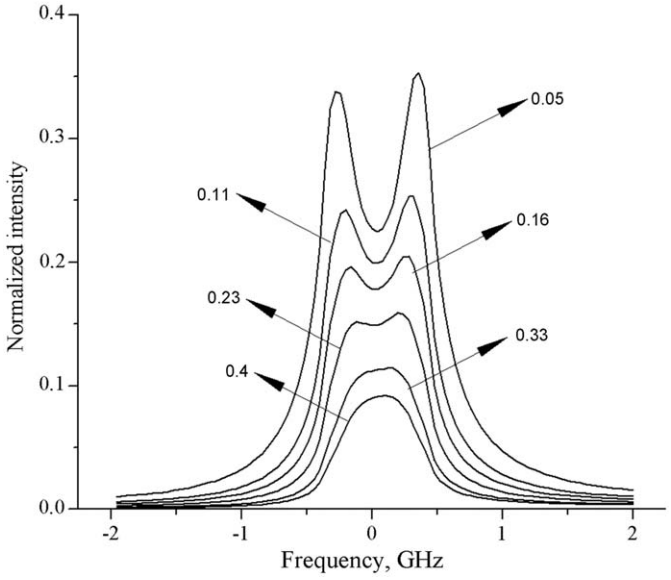

Fig. 2. Spectral dependence of the laser light emitted by the diode laser at the interferometer Output 1 at increasing absorption in the cell with Cs atoms (simulation); the numbers indicate the amplitude transmission of the cell in the center of the Cs line.

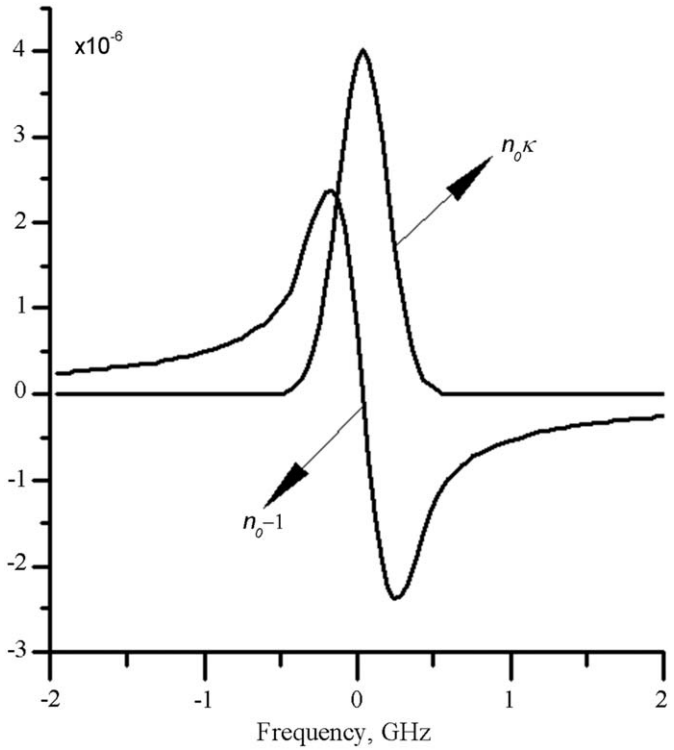

Fig. 3. Calculated frequency dependence of the refractive index and absorption variation throughout the Cs 852.1 nm line at amplitude transmission of the cell $\tau(\nu_0) = 0.05$ in the center of the line (see Eq. (3)).

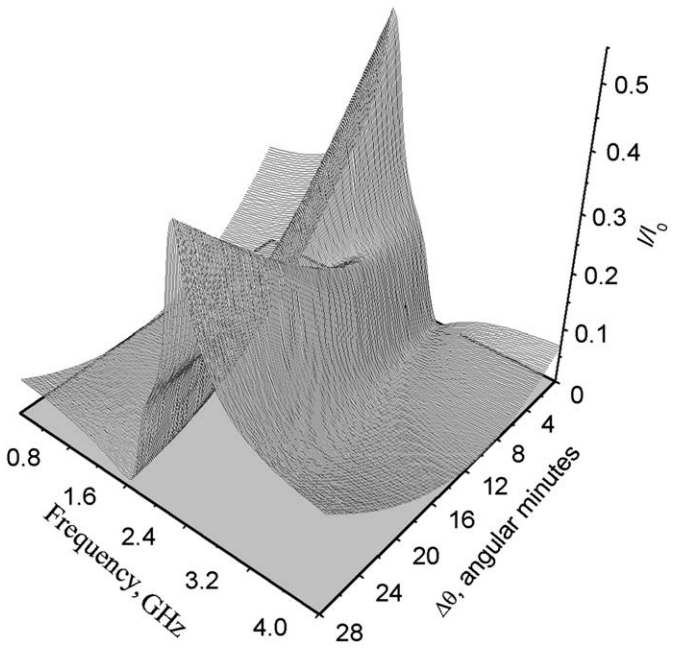

Fig. 4. Spectral dependence of the laser light emitted by the diode laser at the interferometer Output 1 as a function of the inclination angle of the glass plate with respect to the laser beam propagation (simulation); the amplitude transmission of the cell in the center of the line is 0.11.

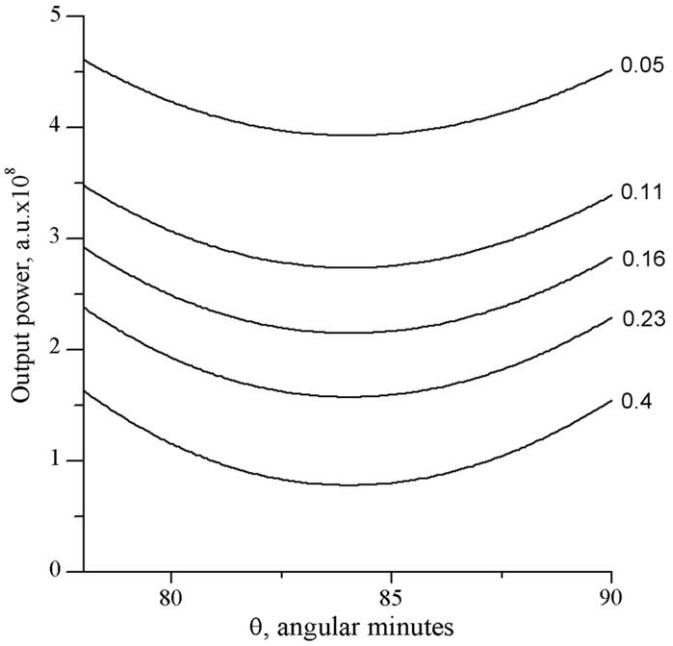

Fig. 5. Total power $P(\theta) = \int_{\nu_1}^{\nu_2} I(\nu)/I_0 d\nu$ at the interferometer output within the spectral interval of $\nu_2 - \nu_1 = 4$ GHz as a function of θ (simulation); the numbers indicate the amplitude transmission of the cell in the center of the Cs line.

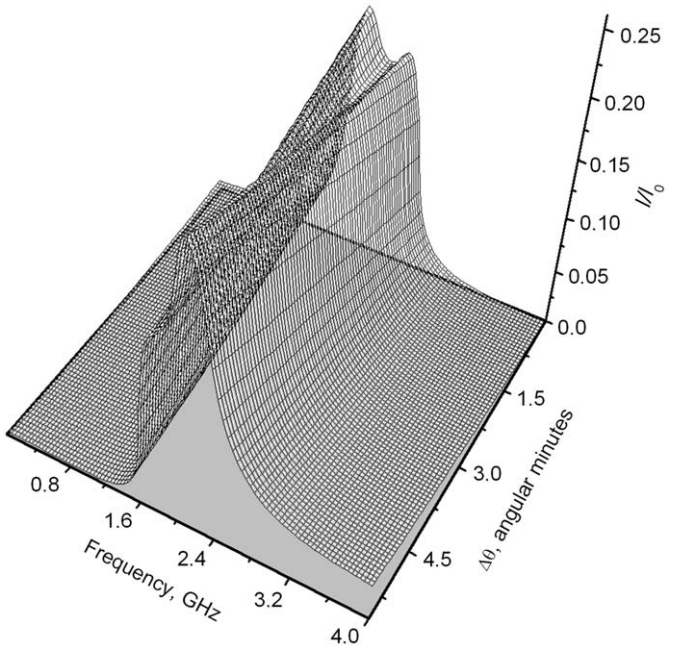

Fig. 6. Spectral dependence of the laser light emitted by the diode laser at the interferometer Output 1 as a function of the inclination angle of the glass plate with respect to the laser beam propagation (simulation); the amplitude transmission of the cell in the center of the line is 0.16.

remains practically constant within 4–5 angular minutes around the minimum. The spectral dependence of the output intensity within this interval is shown in Fig. 6 for $\tau(\nu_0) = 0.16$. It is interesting to evaluate the spectral width of the system output as a function of absorption within the cell with Cs atoms. This dependence is depicted in Fig. 7 (top), where the X axis corresponds to amplitude absorption in the center of the line. Fig. 7 (bottom) shows the ratio between the output power $P(\theta) = \int_{\nu_1}^{\nu_2} I(\nu)/I_0 d\nu$ evaluated for the optimal value of the angle θ only within the contour of $I(\nu)/I_0$ and the input power delivered in this spectral interval. We see that there exists an optimal absorption at which the system output reaches its maximum value. We may

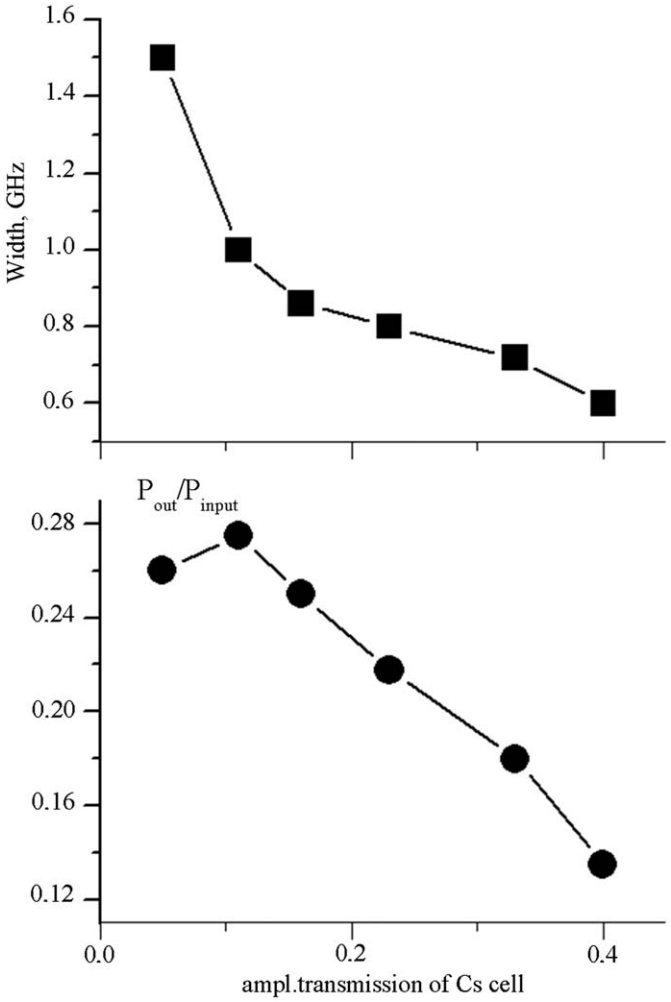

Fig. 7. Spectral width of the laser light emitted by the diode laser at the interferometer Output 1 (top) and the ratio between the output power and input power delivered within the spectral interval of the output intensity $I(\nu)/I_0$ (bottom) as a function of the amplitude absorption in the center of the line.

conclude from the results of the simulation that (i) the proposed laser system can emit radiation with a spectral width of the order of 1 GHz and (ii) it exhibits stable operation allowing for misalignment of the introduced glass plate of several angular minutes.

4. Experimental verification

The experimentally obtained plots of the laser output demonstrated the described interference phenomenon when scanning over a large spectral range, covering a few tens GHz (about 0.016 nm). An example of the laser output is shown in Fig. 8, where the top curve corresponds to the Mickelson interferometer Output 1 (the signal from the diode PhD_1) while the bottom curve depicts the signal from the diode PhD_2 (inverse polarity) that gives the absorption by the Cs line in the external reference Cs cell. The increase in the interferometer output which is correlated with the spectral position of the Cs line is clearly seen in the right part of the top curve in Fig. 8. By tilting the glass plate, an optimized compensation between the refractive indices in both arms can be achieved and a single spectrally fixed line can be produced. The absorption within the line leads to an additional increase of the power at Output 1, especially at the absorption line center.

Three typical cases of emission control performed by varying the angular position of the glass plate are shown in Fig. 9. The

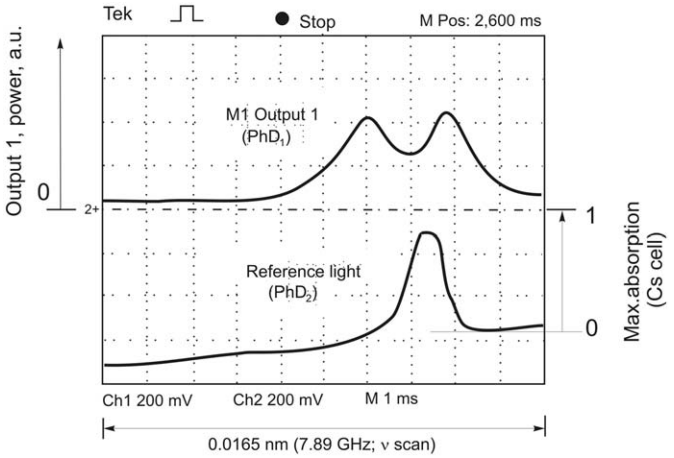

Fig. 8. Spectrograms of the laser light emitted by the diode laser at the interferometer Output 1 (top) and after passing the external reference Cs cell (bottom; inverted polarity) for the diode laser frequency scanned within a given interval.

curves of the laser line and the reference line (represented with inverse polarity) have notations A and B, respectively. Both curves are superimposed in figures. The top picture (Fig. 9a) shows the spectral fixation under strongly non-optimized conditions. In this case, the emission spectrum consists of two peaks of more or less comparable height. By further inclining the glass plate by a few angular minutes, an optimum position is achieved and the emitted output transforms into a single line (Figs. 3b and c). As it is seen in the non-optimized case, the intersection area of the two curves comprises approximately one third of the surface restricted by each curve and the spectrum of the laser emission covers a relatively large spectral range. For the optimized conditions (Fig. 3c), a linewidth of ~1.7 GHz (0.0035 nm) is achieved that is comparable to the measured width of the reference line B (0.9 GHz, 0.0019 nm). The intersection area of the two curves approaches 50% of the surface restricted by each curve. The performance of the optical arrangement is completely reproducible and is characterized with good long-term stability (~hours). As we showed in simulation (Fig. 6), the emitted power is practically constant for misalignments of a few angular minutes, so the set-up could be considered stable with respect to inevitable mechanical vibrations. In our experimental arrangement, we achieved accuracy of 20 MHz rms of intensity peak spectral position. The output power comprises ~20% of the diode laser emission power. Note that a very important requirement for successful operation of the described arrangement is the exclusion of the parasitic feedback for the diode laser. Any non-controlled scattering in the optical elements of the scheme can produce such a feedback. The use of a Faraday isolator could guarantee the successful operation of the system. However, we applied much cheaper isolation in our experiment by mounting a polarizer and a quarter-wave plate in front of the diode laser. The obtained results proved that for the used interferometer, placed at 2 m from the diode laser, the introduced isolation was completely sufficient, provided a careful alignment was maintained and two 1 mm hole diaphragms were used. The final result is ~2 mW light power at the Output 1 for ~10 mW emitted power of the diode laser.

5. Conclusion

In conclusion, we have described a simple, low-cost and purely optical arrangement to produce a diode laser emission, spectrally

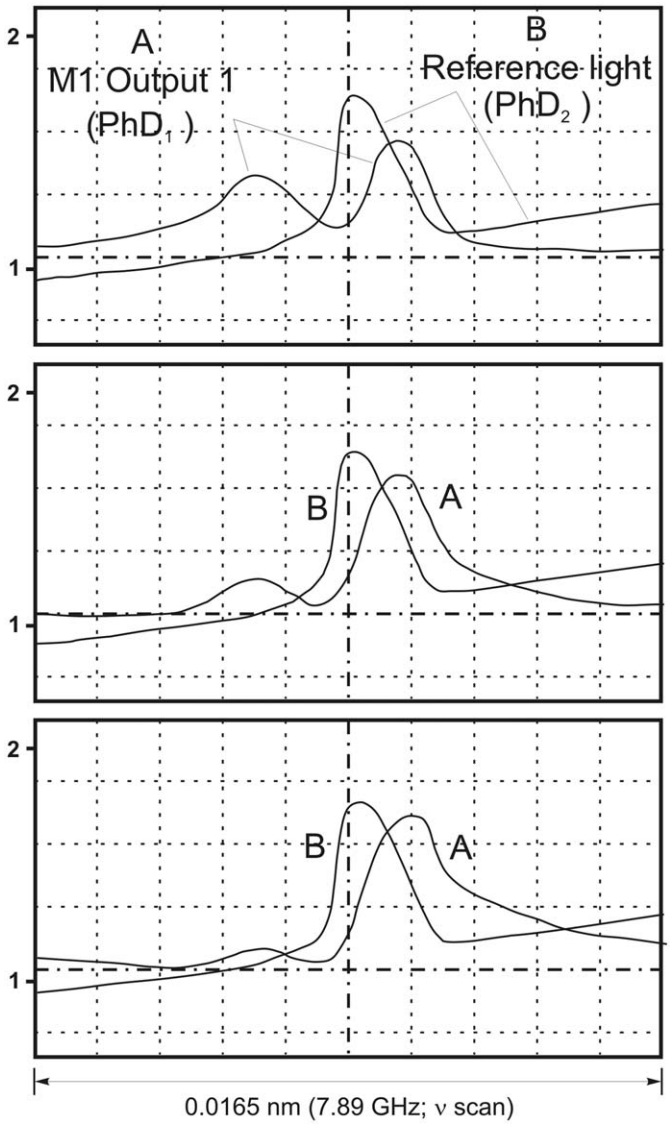

Fig. 9. Spectrograms of the diode laser light emitted at the Output 1 (curve A) and after passing the external reference Cs cell (curve B, inverted polarity) for the diode laser frequency scanned within a given interval. The three figures (a)–(c) correspond to three different angular positions of the glass plate (the change of the angle θ from (a) to (c) is within a few angular minutes); (c) shows the obtained optimal spectral fixation condition.

fixed at a desired atomic absorption line. The reported technique differs from the well-known "laser locking" type approaches characterized with a complicated intra- or extra-resonator influence on the laser operation. Quite the contrary, no influence is performed on the laser operation in the proposed approach which implements external spectrally selective interferometric control of emission from a conventional diode laser. The spectral scanning around the absorption line is achieved by changing the diode driving current. We have found conditions which ensure that the obtained laser emission is practically a single line; its spectrum is fixed to the desired transition, but slightly shifted from its central frequency to the shorter wavelengths. In the realized experimental set-up, the spectral fixation was demonstrated on the example of the Cs 852.1 nm line. The obtained output spectrum in this case was characterized with FWHM of 0.0035 nm, whereas the linewidth of the Doppler-broadened transition was 0.0019 nm; the intersection area of the two curves reached 50% of the surface restricted by each curve. The output power was ~20% of the diode laser emission power. The reported technique can be useful in variety of spectroscopic applications when the target is a single transition which should be excited to monitor or separate a particular substance from a mixture of different substances.

The analysis of the system operation, based on the classical atomic model, is in good agreement with the experimental results. The theory confirms that such control of a diode laser emission is completely realizable. Moreover, the calculations prove that a deviation of the glass plate from the chosen position of the order of a few angular minutes is not critical for the system operation. In practice, we observed better overlap of the absorption and generation curves than is predicted by the theory, which could be related to the accepted simplifications in the theoretical consideration.

Acknowledgments

This work was supported by the Laboratoire de Physique des Lasers, Universite Paris-Nord, France, and partially by the NSF Bulgaria (Contract VUPh 12). M.D. and M.N. thanks the Laboratoire de Physique des Lasers for the kind invitation.

References

[1] Park H, Kwon D, Rhee Y. High-resolution spectroscopy of Sm I performed with an extended-cavity diode laser. J Opt Soc Am B 2004;21:1250–4.
[2] Olson A, Carlson E, Mayer S. Two-photon spectroscopy of rubidium using a grating-feedback diode laser. Am J Phys 2006;74(3):218–23.
[3] Cundiff S, Ye J, Hall J. Optical frequency synthesis based on mode-locked lasers. Rev Sci Instrum 2001;72(10):3749–70.
[4] Moon H. Frequency stabilization of a 1.3 μm laser diode using double resonance optical pumping in the 5P3/2–6S1/2 transition of Rb atoms. Appl Opt 2008;47:1097–102.
[5] Chui H-C, Ko M-S, Liu Y-W, Lin T, Shy J-T, Shaw S-Y, et al. Frequency stabilization of a frequency-doubled 197.2 THz distributed feedback diode laser on rubidium 5S1/2→7S1/2 two-photon transitions. Opt Laser Eng 2006;44:479–85.
[6] Olivares I, Duarte A, Saravia E, Duarte F. Lithium isotope separation with tunable diode lasers. Appl Opt 2002;41(15):2973–7.
[7] Zhao Y. Signal-induced fluorescence in photomultipliers in differential absorption lidar systems. Appl Opt 1999;38:4639–48.
[8] Wang Y, Peng C, Zhang H, Le H. Wavelength modulation imaging with tunable mid-infrared semiconductor laser: spectroscopic and geometrical effects. Opt Express 2004;12:5243–57.
[9] Patrick H, Wieman C. Frequency stabilization of a diode laser using simultaneous optical feedback from a diffraction grating and a narrowband Fabry-Perot cavity. Rev Sci Instrum 1991;62:2593–5.
[10] Leo D, Cambell J. Optically stabilized AlxGa1–x/GaAs laser using magnetically induced birefringence in Rb vapor. Appl Phys Lett 1992;58(10):995–7.
[11] Loe-Mie R, Papoyan AV, Akulshin AM, Lezama A, Rios Leite JR, Lopez O, et al. Nearly all-optical frequency-stabilization of a laser diode on the 120 kHz intercombination line of Ba. J Opt Commun 1997;139:55–9 [and references therein].
[12] Muller R, Weis A. Laser frequency stabilization using selective reflection spectroscopy. Appl Phys 1998;B 66:323–6.
[13] Kozuma M, Kourogi M, Ohtsu M, Hori H. Frequency stabilization, linewidth reduction, and fine detuning of a semiconductor laser by using velocity-selective optical pumping of atomic resonance line. Appl Phys Lett 1992; 61(16):1895–7.
[14] Balushev S, Friedman N, Khayakovich L, Carasso D, Johns B, Davidson N. Tunable and frequency-stabilized diode laser with a Doppler-free two-photon Zeeman lock. Appl Opt 2000;39(27):4970–4.
[15] Poulin M, Latrasse C, Touahri D, Tetu M. Frequency stability of an optical frequency standard at 192.6 THz based on a two-photon transition of rubidium atoms. Opt Commun 2002;207:233–42.
[16] Shin C, Ohtsu M. Stable semiconductor laser with a 7 Hz linewidth by an optical–electrical double-feedback technique. Opt Lett 1990;15(24):1455–7.
[17] Zhao YT, Zhao JM, Huang T, Xiao LT, Jia ST. Frequency stabilization of an external-cavity diode laser with a thin Cs vapour cell. J Phys D: Appl Phys 2004;37:1316–18.
[18] Jitschin W. Locking the laser frequency to an atomic transition. Appl Phys 1984;B:33:7–8.
[19] Li RN, Jia ST, Bloch D, Ducloy M. Frequency-stabilization of a diode laser with ultra-low power through linear selective reflection. Opt Commun 1998;146: 186–8.

[20] Talvitie H, Merimaa M, Ikonen E. Frequency stabilization of a diode laser to Doppler-free spectrum of molecular iodine at 633 nm. Opt Commun 1998; 152:182–8.
[21] Slavov D, Deneva M, Stoykova E, Nenchev M, Barbe R, Keller JC. Output control of a ring laser using bi-directional injection: a new approach for unidirectional generation at a reference atomic absorption line. Opt Commun 1998; 157:343–51.
[22] Deneva M, Nenchev M, Barbe R, Keller JC. Unidirectional ring Ti:Al_2O_3 laser generation at the wavelength of an atomic absorption line by bi-directional passive self-injection locking. Appl Phys Lett 2000;76(10):131–3.
[23] Bernard JE, Marmet L, Madej AA. A laser frequency lock referenced to a single trapped ion. Opt Commun 1998;150:170–4.
[24] Corwin KL, Lu ZT, Hand CF, Epstein RJ, Wieman CE. Frequency-stabilized diode laser with the Zeeman shift in an atomic vapor. Appl Opt 1998;37: 3295–3298.
[25] Yashchuk VV, Budker D, Davis JR. Laser frequency stabilization using linear magneto-optics. Rev Sci Instrum 2000;71(2):341–6.
[26] Clifford MA, Lancaster GPT, Conroy RS, Dholakia K. Stabilization of an 852 nm extended cavity diode laser using the Zeeman effect. J Mod Opt 2000; 47(11):1933–40.
[27] Wasik G, Gawlik W, Zachorowski J, Zawadzki W. Laser frequency stabilization by Doppler-free magnetic dichroism. Appl Phys B 2002;75:613–19.
[28] Petelski T, Fattori M, Lamporesi G, Stuhler J, Tino GM. Doppler-free spectroscopy using magnetically induced dichroism of atomic vapor: a new scheme for laser frequency locking. Eur Phys J D 2003;22:279–83.
[29] Hori H, Kitayama Y, Kitano M, Yabuzaki T, Ogawa T. Frequency stabilization of GaAlAs laser using a Doppler-free spectrum of the Cs-D2 line. IEEE J Quantum Electron 1983;QE-19:169–75.
[30] Shevy Y, Deng H. Frequency-stable and ultranarrow-linewidth semiconductor laser locked directly to an atomic-cesium transition. Opt Lett 1998; 23(6):472–4.
[31] Fukuda K, Farukawa M, Hayashi S, Tachikawa M. Frequency stabilization of a diode laser with a thin Cs-vapor cell. IEEE Trans Ultrason, Ferroelectr Freq Control 2000;47(2):502–5.
[32] Gazazyan EA, Papoyan AV, Sarkisyan D, Weis A. Laser frequency stabilization using selective reflection from a vapor cell with a half-wavelength thickness. Laser Phys Lett 2007;4(11):801–8.
[33] Crance M, Juncar P, Pinard J. A new method for measuring relative oscillator strengths using a cw dye laser. J Phys B, A Mol Phys 1975;8:246–9.
[34] Bonsch G, Potulski E. Measurement of the refractive index of air and comparison with modified Edlem's formulae. Metrologia 1998;35:133–9.
[35] Demtroder W. Laser spectroscopy, 3rd ed.. Berlin Heidelberg New York: Springer; 2003.
[36] Born M, Wolf E. Principles of optics, 6th ed.. Oxford: Pergamon Press Ltd.; 1980.
[37] Libbrecht K, Libbrecht M. Interferometric measurement of the resonant absorption and refractive index in rubidium gas. Am J Phys 2006; 74(12):1055–61.
[38] Li R, Jia S, Bloch D, Ducloy M. Frequency-stabilization of a diode laser with ultra-low power through linear selective reflection. Opt Commun 1998; 146:186–8.